PID controllers and anti-windup systems tuning using ant colony optimization

Maude-Josée Blondin and Pierre Sicard
Groupe de Recherche en Électronique Industrielle, Université du Québec à Trois-Rivières
Trois-Rivières (Québec), Canada
Tel.: +1 (819) – 376-5011.
Fax: +1 (819) – 376-5219.
E-Mail: MaudeJosee.Blondin@uqtr.ca; Pierre.Sicard@uqtr.ca
URL: http://www.grei.ca

Acknowledgements

This work was supported by a fellowship and a research grant from the Natural Sciences and Engineering Research Council of Canada.

Keywords

Optimisation, Motion control, Active damping, Autotuning, DC machine, Non-linear control

Abstract

Ant Colony Optimization allows simultaneous tuning of a large number of control parameters and provides flexibility in the choice of the performance criterion. An off-line tuning methodology is proposed for PID-type controllers and their associated anti-windup subsystem for cascaded loop control structures. Insight is given on the design process, on parameter setting and on handling of soft and hard constraints. The method is illustrated by tuning a weighted PID controller and saturation management for a positioning axis in a grinder application.

1. Introduction

Many methods and rules (lambda tuning, Ziegler-Nichols, frequency response methods, heuristic methods, etc.) have been proposed for tuning Proportional-Integral-Derivative (PID) controllers, either to obtain initial setting of their parameters or for fine tuning [1]. The tuning rules are typically defined for the basic (ideal) PID controller or for controllers with a specific factorization or form. Moreover, the rules typically respond to particular performance criteria (Integral of Absolute value of Error (IAE), Integral of Squared Error (ISE), Integral of Time multiplied by the Absolute value of Error (ITAE), etc.) and do not take into account controller saturation. Rules also do exist to tune anti-windup controllers and it is customary to sequentially tune the PID and the anti-windup controllers. However, there exists close interaction between controller and anti-windup tuning. It was noted that the sequential approach is not efficient [2], [3]. In fact, it may lead to sluggish performance, henceforth the interest of using a more global approach, which can handle a large set of parameters, to tune adequately and simultaneously the PID system with anti-windup. Moreover, in order to manage more realistically the system, it would be relevant to have a tuning method with a flexible performance criterion that takes into account system limitations and constraints.

In [4], Ant Colony Optimization (ACO) has been proposed to tune PID controllers. We have used ACO as an offline tuning method [3] and we observed that this method offers several advantages. Firstly, tuning may be controller-structure independent. It also allows considering variations of the structure of the controller, such as tuning of input filters, fractional-order controllers, etc. Moreover, performance criterion is not fixed and does not require an analytic solution so that specific behaviours such as overshoot can be specifically penalized. Cascaded control loops may also be tuned simultaneously; in particular when time scale separation is not sufficient, which results into a large number of interdependent parameters to be tuned.

In industrial applications, it is common that the system has to cope with disturbances while responding correctly to a desired set point. It is a challenge to provide satisfactory response to both these inputs with a classical PID controller and additional degrees of freedom are needed for stringent performance requirements. With its added degrees of freedom, the weighted PID controller provides globally better results for step response and step disturbance than the PID controller.

In this paper, we propose an ACO based methodology applied to a motion system with flexible coupling for tuning cascaded loops control structures with saturation. We show the efficiency of ACO to tune simultaneously: the weighted position loop PID controller with filtered derivative term (PID_f); its anti-windup feedback gain and the anti-windup gain of the current control loop. Furthermore, through an appropriate choice of the performance criterion, we demonstrate the flexibility provided by our method, e.g. to impose hard or soft current and motor velocity limitation, or to penalize specific behaviours such as output overshoot.

2. Ant Colony Optimization

ACO is an optimization technique inspired by the behaviour of real ants within a colony [5] [6]. It was observed that a colony facing multiple paths to a food source has the tendency of taking the shortest road. This is explained by the fact that ants communicate with each other via their environment by depositing traces of pheromones. The paths with the most pheromones are more attractive to other ants. Therefore, the amount of pheromones increases more rapidly on the shortest path, attracting more and more ants. Eventually, all ants will take the same path, i.e. the shortest path. Henceforth, the solution emerges from the collective interaction of the ants.

ACO can be used to solve combinatorial optimization problems for which a constructive heuristic can be employed. One of the first problems ACO was applied to is the Traveling Salesman Problem (TSP), which allows illustrating the method. The ants move on the TSP graph and generate different solutions. The probability for an ant k located in city i to choose city j is stated as

$$P_{ij}^{k}(t) = \frac{[\tau_{ij}(t)]^{\alpha}[\eta_{ij}(t)]^{\beta}}{\sum_{l \in N_i^k} [\tau_{il}(t)]^{\alpha}[\eta_{il}(t)]^{\beta}} \tag{1}$$

where N_i^k represents the number of cities to be visited by the ant k, $j \in N_i^k$; $\tau_{ij}(t)$ is the quantity of pheromones deposited between cities i and j; $\eta_{ij}(t) = 1/d_{ij}$ is the inverse of the distance separating cities i and j; α and β are parameters that determine respectively the relative weight of pheromone traces and the heuristic information.

At each step, each ant deposits pheromones on its travelled path:

$$\tau_{ij}(t+1) = \tau_{ij}(t) + \sum_{k=1}^{m} \Delta\, \tau_{ij}^{k}(t) \;\forall\, (i,j) \in L \tag{2}$$

where $\Delta\, \tau_{ij}^{k}(t)$ is the quantity of pheromones deposited on segments that ant k has visited during this step. The quantity of deposited pheromones on each segment of the graph is function of the quality of the solution:

$$\Delta\, \tau_{ij}^{k}(t) = \begin{cases} 1/L^{k} & \forall\, (i,j) \in L \\ 0 & \text{otherwise} \end{cases} \tag{3}$$

where L is the total length of travelled distance for the iteration. The pheromone traces associated to each segment are reduced by a constant evaporation rate ρ :

$$\tau_{ij} = (1-\rho)\tau_{ij} \;\; \forall\, (i,j) \in L \tag{4}$$

where $0 < \rho < 1$. The evaporation process constitutes a forgetting factor used to avoid unlimited accumulation of pheromones and to allow forgetting previous bad decisions.

3. ACO for PID_f and anti-windup tuning

To demonstrate the tuning methodology, one axis of the positioning table of an industrial grinder

system is considered in this study. A 3/4 hp, 5200 rpm, 3.5 N·m, dc motor is coupled to the grinder table by a gear box and a worm-gear such that 1 rad of motor rotation causes a displacement of 0.1 mm of the grinder table. The significant flexible coupling due to the transmission elements is modelled as an equivalent lumped spring. Performance criteria include high accuracy, minimal overshoot and good dynamic performance to improve product quality, avoid stress on the grinder and decrease the operation cycle. The flexible coupling complexifies the tuning process to achieve high performance for this cascaded loop control system. The typical solution for this type of system is to use cascaded current and table position control loops with an inner motor velocity loop to improve damping and reduce oscillations. Tuning for performance is more challenging than simple cascaded control loops, in particular when considering system constraints such as saturation levels and velocity limitations.

Figure 1 summarizes the system model and ACO's main input and output parameters for controller and anti-windup parameter tuning, which is applied to various cases of system constraints (Figures 2, 3 and 4). The first position controller is illustrated in Figure 2, along with its parameters. It is composed of a PID controller with filtered derivative term, a motor velocity feedback (K_{vel}) and an anti-windup controller. The inner PI current controller was tuned separately but its anti-windup feedback gain K_{satI} (Figure 1) will be tuned by the ACO. Figure 3 presents the structure of the weighted PID_f controller where parameters W_p and W_v represent the weighting factors on the proportional and derivative terms of the PID_f controller, effectively modifying the zeroes of the transfer function from the reference position to the actual grinder table position. Figure 4 shows the last controller structure used where motor velocity limitation is considered instead of current saturation for anti-windup. Both could have been considered simultaneously, but considering that the motor is lightly loaded, its current does not saturate for significant periods and a simple saturator was deemed sufficient for this scheme.

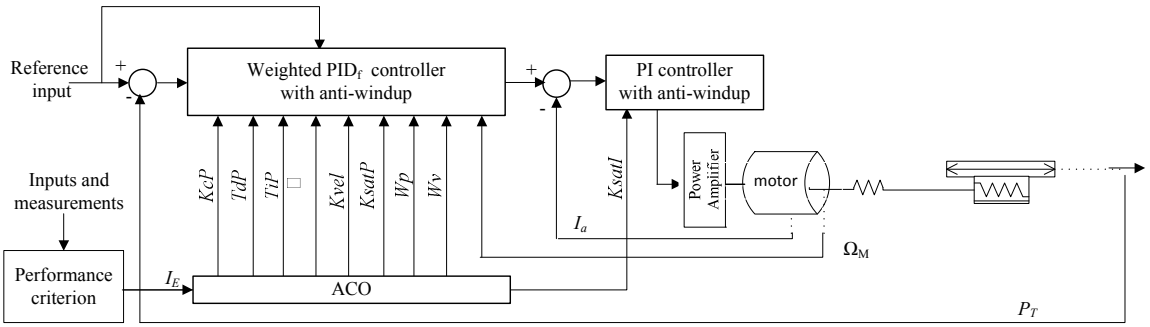

Fig. 1: System overview with ACO application for tuning PID_f and anti-windup system parameters.

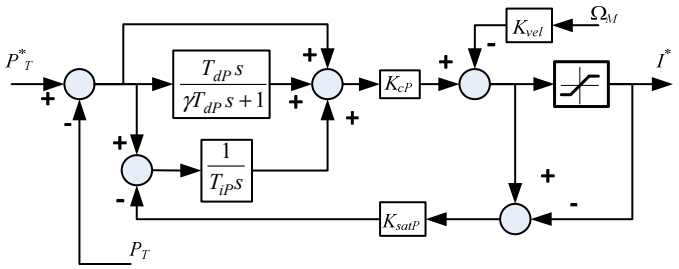

Fig. 2: Position feedback controller and anti-windup scheme.

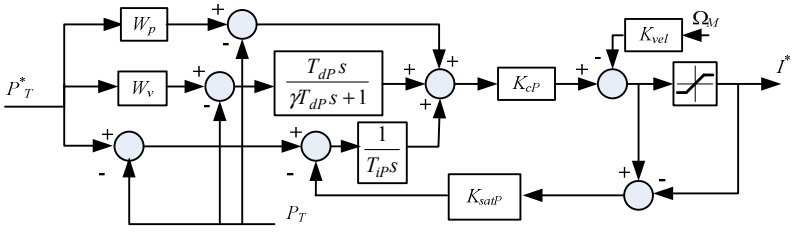

Fig. 3: Weighted PID_f controller structure with anti-windup for current reference limitation.

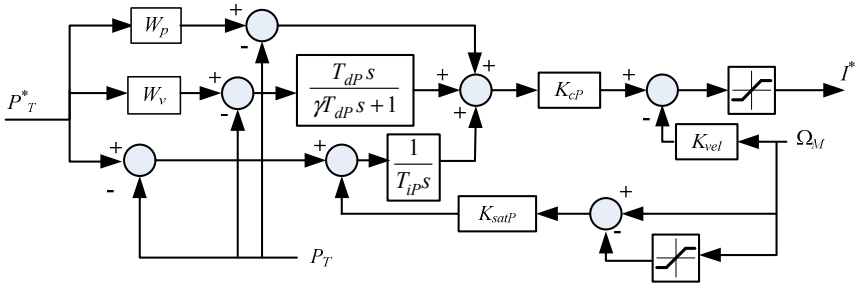

Fig. 4: Weighted PID_f controller structure with anti-windup for motor velocity limitation.

To use ACO, controller tuning must be transformed into a combinatorial optimization problem [4], [7], [8] (Figure 5). Each slice of the graph corresponds to nodes of quantized controller parameters. This representation allows easy addition or removal of free controller coefficients. Range of parameters and quantization steps must be chosen to complete the graph of Figure 5. Rough tuning of the control parameters can be used to define the range of parameters. The ants move on the graph from left to right by choosing the nodes they travel from probabilistic rules. They leave pheromone traces as a function of the quality of the solution (c.f. Section 2).

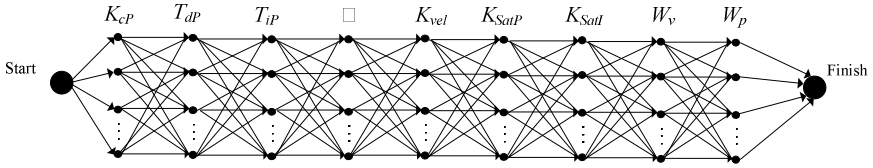

Fig. 5: Optimization graph for weighted PID_f controller and anti-windup coefficients.

The performance is evaluated by I_E index resulting from the set of parameters on the travelled path. The objective of the ACO is to find the best set of parameters to minimize I_E. The choice of the performance criterion is critical to obtain the desired behaviour with regards to transients, steady state and inner variables limitation. To simultaneously consider set point performance and disturbance rejection criteria, a performance index with normalized quantities was defined as follows (some coefficients are set to zero for some of the tests):

$$I_E = \sum\left(\int_{t_s}^{t_s+T_s} \frac{|e(t)|}{\Delta P_T^*}dt\right) + K_t \sum\left(\int_{t_p}^{t_p+T_p} \frac{|e(t)|}{\Delta T_{pert}}dt\right) + \sigma\int_0^{T_f} \frac{e_d(t)}{\Delta P_T^*}dt + \beta\int_0^{T_f} \frac{e_{v_d}(t)}{\Omega_{Mm}}dt \qquad (5)$$

where:

• the first two terms are summations over each of the set point step input and disturbance input transients respectively: t_s is the time of last set point variation; T_s is the approximate settling time for the set point step response; t_p is the time of last disturbance input variation; T_p is the approximate settling time for the step disturbance; $e(t)=P^*_T(t)-P_T(t)$ is the output error; P_T and P^*_T are respectively the measured and reference positions of the grinder table; ΔP^*_T is the amplitude of the last step input variation used to normalize the position error; ΔT_{pert} is the amplitude of the last force disturbance variation; K_t is a positive constant of equivalent stiffness used to normalize the position error due to force disturbance;

• the third term penalizes position overshoots: T_f is the simulation time as this term is penalized continually; σ is a positive constant weight; $e_d(t)$ is defined as

$$e_d(t) = \begin{cases} |e(t)| & \text{during response overshoots} \\ 0 & \text{otherwise.} \end{cases} \qquad (6)$$

• the fourth term penalizes motor velocity limit violations:

$$e_{v_d}(t) = \begin{cases} |\Omega_M(t)| - \Omega_{Mm}| & \text{if exceeding the motor velocity limit} \\ 0 & \text{otherwise} \end{cases} \qquad (7)$$

where Ω_{Mm} is the upper motor velocity limit.

Larger values of σ in (5) penalize more the overshoot, which is very detrimental to the quality of the grinding operations. Larger values of K_t are used to reduce the impact of the disturbance on the system. β is used to constrain the motor speed to respect the system limits. Choice of the weights is analysed in the next section.

4. Simulation Results

The ACO algorithm was implemented in Matlab® and the system's model on Simulink™ to implement off-line parameter tuning (Figure 6). The position PID_f controller's parameters were initially determined by pole placement from the approximate rigid model of the system and the following ranges were chosen for the parameter coefficients for the search (wide ranges were chosen to extend the space of possible solutions):

K_{SatP}: [1 *to* 1000] K_{SatI}: [1 *to* 1000]
K_{cP}: [0.001 *to* 10] T_{iP}: [0.003 *to* 30]
T_{dP}: [0.001 *to* 10] γ: [10 *to* 50]
W_v: [0 *to* 1] W_p: [0 *to* 1]
K_{vel}: [0.01 *to* 0.1]

The number of quantization steps was fixed to 75. The quantization step size was imposed by using even logarithmic spacing between the coefficient values (constant ratio of consecutive values).

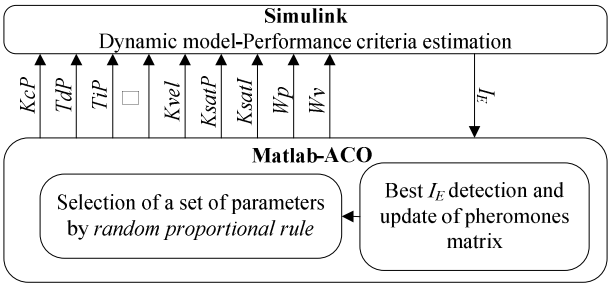

Fig. 6: Simulation environment structure of ACO iteration.

4.1. PIDf controller with current based anti-windup

In a first simulation scenario, the control structure shown in Figure 2 is used. The iteration number for ACO methodology is fixed at 100 and the number of ants to 100. The parameters K_t and β of the performance criteria are set to 0 and no load disturbance is applied. Therefore, the performance criterion is the IAE performance index augmented with an additional term to penalize overshoot. As this characteristic is very detrimental to the grinding operations, decreasing overshoot without reducing dynamic performances is highly desirable. Figure 7 shows the best response obtained by the ACO for $\sigma = 1$. The drive flexibility is observed in the difference between the motor position and scaled grinder table position.

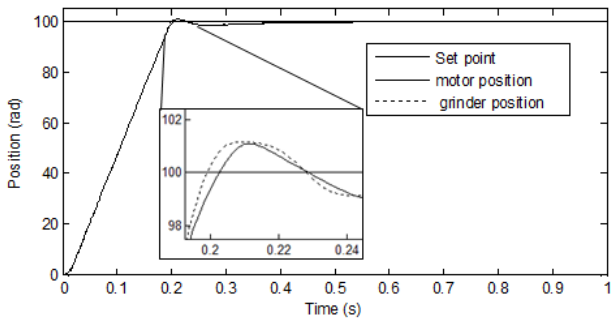

Fig. 7: Step response for PID_f controller for motor position and grinder position using modified IAE index ($\boldsymbol{\sigma = 1}$), with saturation.

Figure 8 compares the grinder position step responses for $\sigma = 1$ and $\sigma = 2$. It substantiates the relevance of using the modified IAE performance index to reduce overshoot.

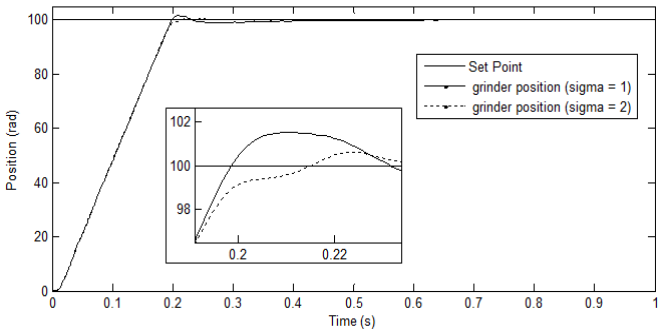

Fig. 8: Step response for the PID_f controller for the grinder position using modified IAE index with saturation.

Figure 9 shows the convergence rate of the algorithm and the best achieved I_E. The average index values decreases with the iterations, as a result of the ants converging towards the best solutions. We notice very little improvement of the best index value after 60 iterations. This means that less than 100 iterations are required to approach optimal tuning of the controller with a good degree of confidence.

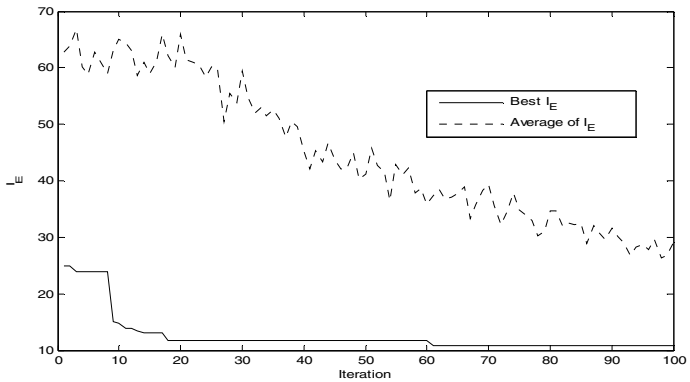

Fig. 9: Convergence rate of the algorithm for set point step response for the modified IAE index ($\boldsymbol{\sigma = 2}$) with saturation.

A step load disturbance corresponding to 20% of the nominal torque (0.75 Nm) and representing a realistic disturbance value is applied to the system at 2 s. Figure 10 shows poor system performance when responding to the disturbance with the parameter values obtained using only the reference input portion of the response.

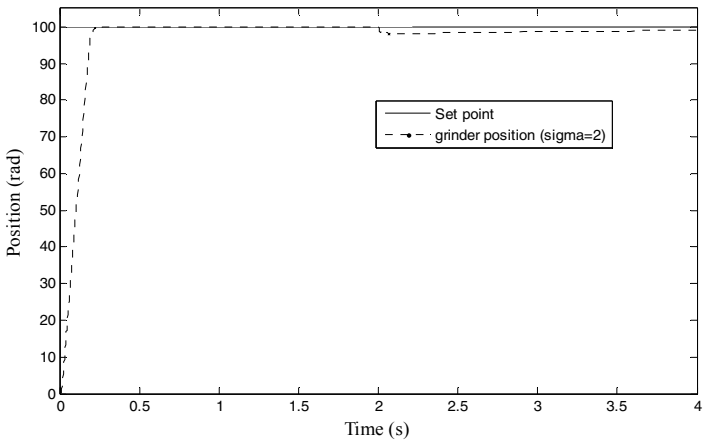

Fig. 10: Step response and step disturbance response for PID_f controller for grinder position using modified IAE index ($\sigma = 2$) evaluated over the first 2 s.

To improve disturbance rejection, coefficient K_t is used in the performance criterion (5) to penalize the output disturbance error. The selection of K_t values is based on the interpretation of the corresponding term in (5) by a spring model and posing a maximum permitted displacement of the grinder table for a given disturbance. From (5), if we write out (this is only an interpretation and the unity factor was used to normalize this term to 1):

$$1 = K_t \frac{|e_{max}|}{\Delta T_{pert}} \tag{8}$$

and assume that for a disturbance of 20% the motor nominal torque, a 1 mm to 0.1 mm of grinder table displacement satisfies (8), the K_t values are respectively 0.075 to 0.75. These values are used as a starting point to eventually "tune" (5). Figure 11 presents the obtained optimal set point step responses and the step load disturbance responses for different K_t values. Figure 11b demonstrates the positive effect of coefficient K_t on improving the disturbance response. On the other side, Figure 11c shows that this was achieved at the cost of a compromise on the transient response to the reference input. Added degrees of freedoms using the weighted PID_f controller and motor velocity limitation management are now introduced to deal with this issue.

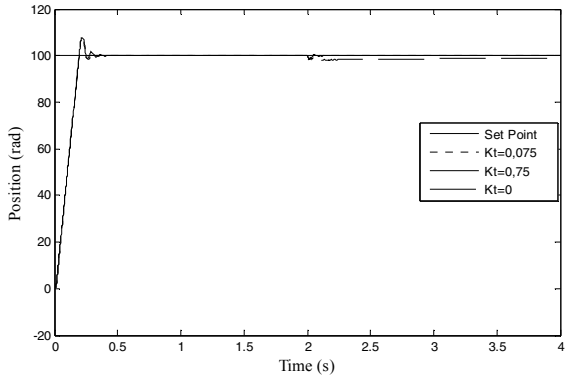

(a) Complete response

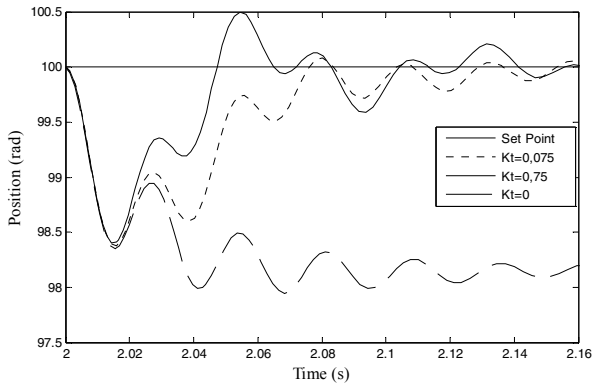

(b) Enlargement of disturbance response

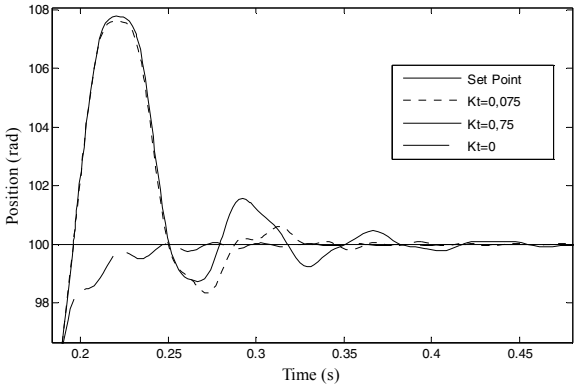

(c) Enlargement of reference input response

Fig. 11: Step response and step disturbance response for PID controller for grinder position ($\sigma = 2$) versus different K_t values.

4.2. Weighted PIDf controller with current based anti-windup

As a second simulation scenario, the control structure shown on Figure 3 is used. The iteration number for ACO methodology is augmented at 200 and the number of ants to 200 due to a larger number of parameters to be adjusted. σ is set to 2 and β is set to 0 in the performance index (5). Coefficients W_p and W_v offer additional degrees of freedom for control so that the controller can simultaneously yield better performance for set point response and disturbance rejection.

Globally, Figure 12 shows better results than those obtained in the first scenario (Figure 11). The weighted controller with K_t =0 improves the input reference step response at the cost of poorer

disturbance rejection, which was expected since the disturbance response was not considered for optimization in this case. For K_t = 0.075, input response has improved and disturbance response is comparable to the previous settings. Improvements are also observed for K_t = 0.75 but with excessive position overshoot (Figures 11c and 12c). This overshoot is due to integrator windup in the position controller due to natural motor velocity saturation as shown on Figure 13.

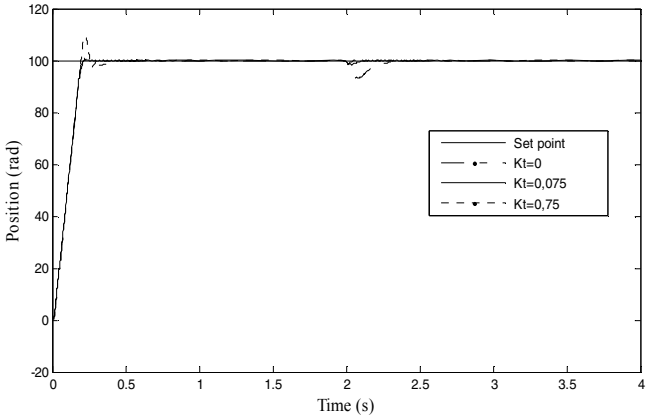

(a) Complete response

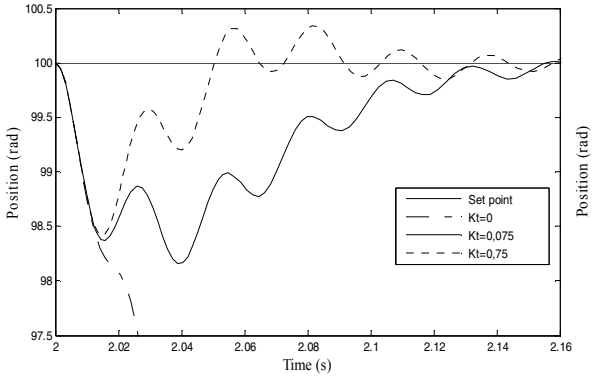

(b) Enlargement of disturbance response

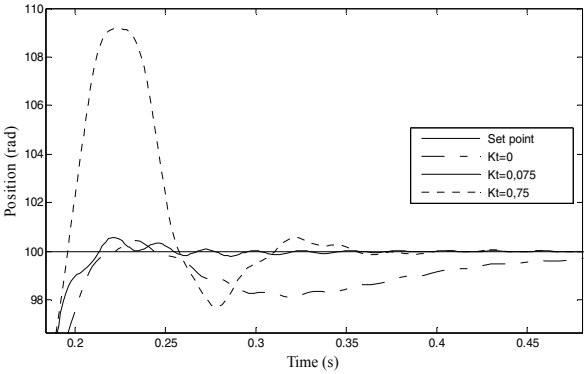

(c) Enlargement of reference input response

Fig. 12: Step response and step disturbance response for weighted PID controller for grinder position ($\sigma = 2$) versus different K_t values.

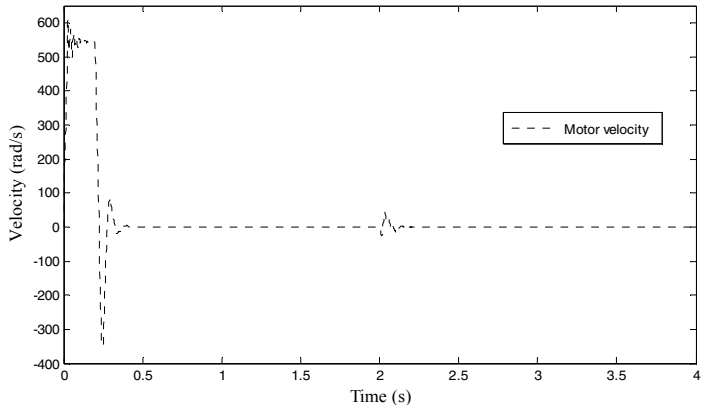

Fig. 13: Motor velocity response; K_t = 0.75 .

4.3. Weighted PIDf controller with motor velocity based anti-windup

In order to improve the overall response, inner limitations must be considered and penalized in the performance index. Henceforth, for the third simulation scenario, the control structure described in Figure 4 is used. We have observed that only including anti-windup feedback based on velocity limitation as illustrated on Figure 4 is insufficient and that it is necessary to explicitly penalize velocity

limit violations (last term in (5)) to obtain the desired effect. Moreover, in order for the response in saturation mode during large input step variations not to dominate in the performance criterion over the small signal operation, a large (100 rad at 0 s) and a small (5 rad at 2 s) input step variations are applied to the system for optimization. A step disturbance corresponding to 20% the motor's nominal torque is applied at 4 s. Parameter β is set to 100 in (5). A larger value of β allows to implement hard constraints on motor velocity, whilst a small value would implement a softer constraint.

Also, in the previous simulation scenarios, overshoot was present. As small as it may be, no overshoot should be present when precision work is required such as in grinding operation. Henceforth, the value of σ is increased to 100 to implement a hard constraint on position overshoot. The iteration number for ACO methodology and the number of ants are still fixed at 200.

Figure 14 show the results obtained when motor velocity limit is set to 386 rad/s and Figure 15 the effectiveness of the performance index to limit the motor velocity. As expected, no position overshoot is present and Figure 14b demonstrates the efficiency of higher K_t values to improve disturbance rejection, eventually at the cost of decreased damping of the transmission's flexibility effects.

These results show that the weighted controller provides a better control over the system response to load disturbances than a PID controller. Also, the ACO method offers flexibility in its performance criterion to adjust the parameters of the controller. This advantage allows to specifically penalising certain aspects of the system behaviour to respect system limitations and to adapt the system to the application.

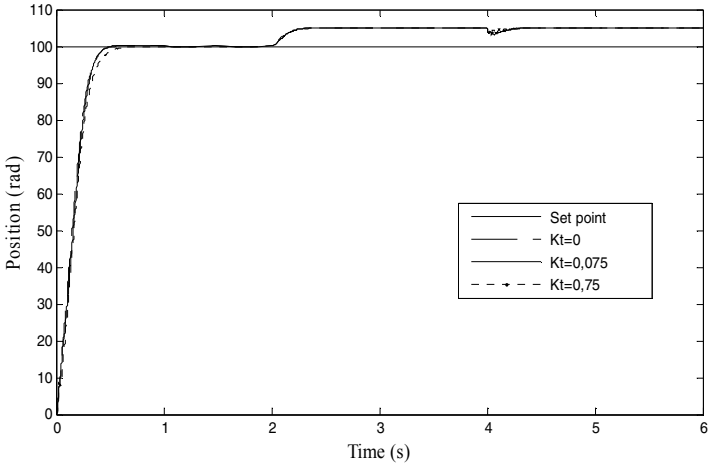

(a) Complete response

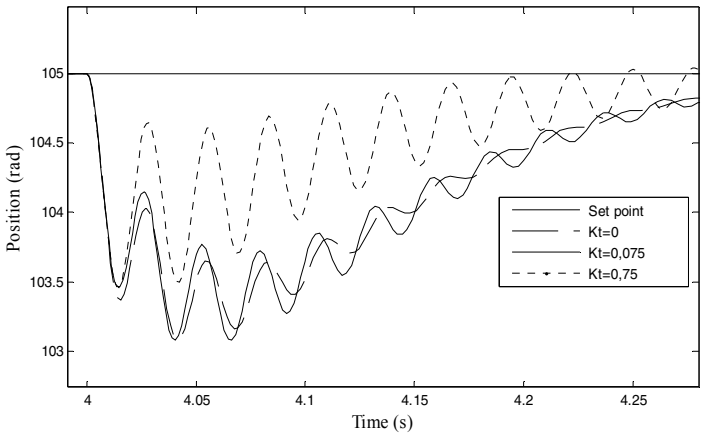

(b) Enlargement of response to disturbance

Fig. 14: Step response with motor velocity saturation for weighted PID_f controller for grinder position versus different K_t values.

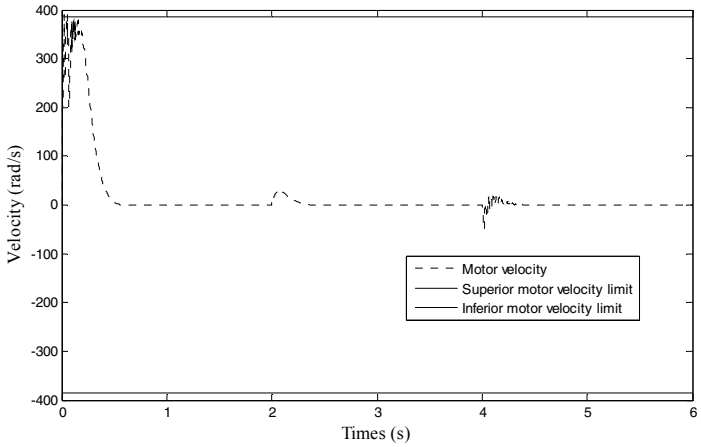

Fig. 15: Motor velocity with saturation compensation; $K_t = 0.075$.

5. Conclusion

Controller tuning in nonlinear systems is a complex task to obtain a satisfactory response to set point and disturbances inputs while respecting the limits of the system and the constraints imposed by the application. The ACO methodology has the advantage of tuning a large number of parameters simultaneously, but also to use a performance criterion tailored to the application. Hard or soft constraints can be imposed by properly choosing the relative weights in the performance criterion. It is also important to choose properly the number of ants and of iterations for the ACO so that the solution is statistically valuable with regards to the number of output parameters and of their quantization. It was also shown that the weighted controller alleviates the need for compromises that must be made between set point response and disturbance rejection. The methodology can be applied to tune industrial systems for which a reasonable model is known. Simulation time may become a problem so that we have initiated work to develop a hybrid algorithm that combines ACO for global search and Nelder-Mead algorithm for controller fine tuning [9].

References

[1] F. Padula, and A. Visioli, “Optimal tuning rules for proportional-integral-derivative and fractional-order proportional-integral-derivative controllers for integral and unstable processes,” Control Theory & Applications, IET, 6(6), pp. 776-786, 2012.

[2] N.J. Killingsworth and M. Krstic, “PID Tuning Using Extremum Seeking,” *IEEE Control Systems Magazine*, pp. 70-79, Feb. 2006.

[3] M.-J. Blondin, and P. Sicard," ACO Based Controller and Anti-Windup Tuning for Motion Systems with Flexible Transmission," *2013 IEEE Canadian Conference on Electrical and Computer Engineering (CCECE’13)*, Regina, Saskatchewan, Canada, 5-8 May 2013.

[4] I. Chiha, N. Liouane, and P. Borne, “Tuning PID Controller Using Multiobjective Ant Colony Optimization,” *Applied Computational Intelligence and Soft Computing*, Hindawi Publishing Corporation, Article ID 536326, 2012.

[5] M. Dorigo, V. Maniezzo, and A. Colorni, “Ant System: Optimization by a Colony of Cooperating Agents,” *IEEE Transactions on Systems, Man, and Cybernetics-part B Cybernetics*, 26(1), pp. 29-41, February 1996.

[6] Dorigo, M., and T. Stützle, *Ant Colony Optimization*, The MIT Press, Cambridge, Massachusetts, 2004.

[7] H.A. Varol, and Z. Bingul, “A New PID Tuning Technique Using Ant Algorithm,” *Proceeding of the 2004 ACC,* Boston, Massachusetts, pp. 2154-2159, June 30 - July 2, 2004.

[8] Y.-T. Hsiao, C.-L. Chuang, and C.-C. Chien, “Ant Colony Optimization for Designing of PID Controllers,” *2004 IEEE ISCACSD*, Taipei, Taiwan, pp. 321-326, September, 2004.

[9] M.-J. Blondin, and P. Sicard,"Combined ACO Algorithm — Nelder-Mead Simplex Search for Controller and Anti-Windup Tuning for a Motion System with Flexible Transmission," submitted to *2013 IEEE 39th Annual Conference of the IEEE Industrial Electronics Society (IECON’13)*, Vienna, Austria, 10-13 November 2013.